Ecological causes of uneven diversification and richness in the mammal tree of life

Short title: Ecological causes of diversification in mammals

Nathan S. Upham[1*], Jacob A. Esselstyn[2], and Walter Jetz[1*]

Author affiliations: [1]Department of Ecology & Evolutionary Biology, Yale University, New Haven, CT 06511 USA. [2]Department of Biological Sciences and Museum of Natural Science, Louisiana State University, Baton Rouge, LA 70803 USA.

*Corresponding authors: 165 Prospect St., OML 122, New Haven, CT 06511 USA; nathan.upham@yale.edu; walter.jetz@yale.edu

Abstract

The uneven distribution of species in the tree of life is rooted in unequal speciation and extinction among groups. Yet the causes of differential diversification are little known despite their relevance for sustaining biodiversity into the future. Here we investigate rates of species diversification across extant Mammalia, a compelling system that includes our own closest relatives. We develop a new phylogeny of nearly all ~6000 species using a 31-gene supermatrix and fossil node- and tip-dating approaches to establish a robust evolutionary timescale for mammals. Our findings link the causes of uneven modern species richness with ecologically-driven variation in rates of speciation and/or extinction, including 24 detected shifts in net diversification. Speciation rates are a stronger predictor of among-clade richness than clade age, countering claims of clock-like speciation in large phylogenies. Surprisingly, speciation rate heterogeneity in recent radiations shows limited association with latitude, despite the well-known increase in species richness toward the equator. Instead, we find a deeper-time association where clades of high-latitude species have the highest speciation rates, suggesting that species durations are shorter (turnover is higher) outside than inside the tropics. At shallower timescales (i.e., young clades), diurnality and low vagility are both linked to greater speciation rates and extant richness. We suggest that high turnover among small-ranged allopatric species has erased the signal of vagility in older clades, while diurnality has adaptively promoted lineage persistence. These findings highlight the underappreciated joint roles of ephemeral (turnover-based) and adaptive (persistence-based) processes of diversification, which manifest in recent and more ancient evolutionary radiations of mammals to explain modern diversity.

Keywords

Phylogenetics, macroevolution, dispersal, mass extinction

Author Summary

The over 6000 living species in the mammalian tree of life are distributed unevenly among branches so that similarly aged groups sometimes differ many fold in species richness (e.g., ~2500 rodent species versus 8 pangolins). Why differential bursts of species diversification occur, and how long they persist, has implications for sustaining biodiversity. Here we develop a robust evolutionary timescale for most extant species, recovering signatures of rate-variable diversification linked to ecological factors. Mammals with low dispersal or that are day-active show the fastest recent speciation rates, consistent with mechanisms of allopatric isolation and ecological opportunity, respectively. Speciation is surprisingly faster in extra-tropical than tropical lineages, suggesting that longer species durations for tropical lineages underpin the latitudinal diversity gradient in mammals.

Introduction

Branches in the mammal tree of life range from mega-diverse rodents and bats to similarly old, yet species-poor, groups like treeshrews and pangolins (stem ages all ~60-70 million years ago [Ma]). Questioning why some evolutionary groups are more speciose than others traces to the classic 'hollow curve' observation of Willis [1], which was formalized for phylogenetic tree shape as unevenness (or imbalance) [2]. Uneven species richness implies uneven net diversification (speciation – extinction), but whether speciose clades usually derive from faster rates or older ages is controversial [2–4]. Similarly debated are the causal roles of environmental factors [3,5–7] or intrinsic traits of species [8,9] as determinants of rate-variable diversification. Recently, analytical advances in identifying macroevolutionary rate regimes [10] and species-level rate variation at the instantaneous present (e.g., the tip DR metric [11,12]) have uncovered gradients of higher speciation rates with latitude [13–15] and elevation [7]. Ephemeral speciation processes [16] appear to underlie these dynamics, where unstable environments produce many short-lived species via high rates of lineage turnover (speciation + extinction). In contrast, adaptive processes that involve accessing novel ecospace are expected to decrease extinction rates [6,17,18], so that species accumulate via persistence not turnover. If nascent allopatric species form regularly [19], then identifying which factors cause them to persist or go extinct (e.g., climate seasonality, dispersal ability, niche adaptations; [7,13,14,16,19–21]) is central to understanding why evolutionary tree shapes and geographic diversity are uneven. The challenge to reconstructing species birth and death across Mammalia is that a robust evolutionary timescale is required for any test of rate variation to be meaningful.

Until now, the species-level phylogenies of mammals have been inadequate for the task of understanding macroevolutionary tree shape. Parsimony supertrees [22] were first

implemented on large scales across Mammalia (Bininda-Emonds et al. [23] and its updates [24,25]). However, supertree methods inherently result in node conflict when merged source trees disagree (e.g., >50% of nodes [23,24]) that, when secondarily resolved [25], add branch length artifacts to regions of the tree with the greatest phylogenetic uncertainty. Supertrees are thus poorly suited for studying rates of lineage diversification (*SI Appendix*, Fig. S14 for a comparison of tree shapes). However, they continue to be a popular choice for large-scale tests of diversification-rate hypotheses [e.g., 26–29]. Herein, we abandon the supertree paradigm, using instead a single DNA supermatrix to improve upon the Bayesian backbone-and-patch approach developed in birds [11], squamates [30], and amphibians [31].

Our goals are to: (i) build sets of species-level mammal phylogenies that are optimized for root-to-tip comparisons of lineage diversification and trait evolutionary rates; (ii) test for tree-wide and among-clade variation in rates through time; and (iii) evaluate the ecological causes of those rate-variable processes, which we find are the primary predictors of species richness among mammal clades. Due to the rapid innovations in phylogenetic comparative methods and frequent controversies over their implementation [e.g., 32–37], we employ multiple modeling strategies at each analysis stage to corroborate our results. Testing for ecological effects on recent versus older radiations reveals complex and age-dependent connections between clade traits, speciation rates, and species richness. We paradoxically find that extant lineages outside the tropics have faster rates of recent speciation than do tropical lineages where modern species richness is the greatest. This type of mismatch suggests that high lineage turnover characterizes larger swaths of the mammal tree of life than previously appreciated—complementing traditionally invoked mechanisms of 'key innovations' [38] and disparate ecological opportunity [6,17,18] to explain uneven species richness patterns.

Results and Discussion

Our mammal tree (Fig. 1) includes 5,804 extant and 107 recently extinct species in a credible set of 10,000 trees, integrates age and topological uncertainty, and incorporates 1,813 DNA-lacking species using probabilistic constraints. It thereby offers a species-level phylogeny with all branches estimated under a unified birth-death framework (available at vertlife.org). Trees are built using: (i) an updated taxonomy; (ii) a newly assembled 31-gene supermatrix; and (iii) the backbone-and-patch approach, which here estimates the phylogenies of 28 mammal subclades (identified in a global DNA tree) with relative branch lengths, re-scales the branches to corresponding divergence times in fossil-calibrated backbones, and grafts each subclade to the backbone (Fig. 2; *Methods*, *SI Appendix*, Datasets S1-S6). We developed four credible sets of Mammalia-wide trees based on node- or tip-dated backbones [39,40] and the inclusion or exclusion of DNA-lacking species. Analyzing samples of trees from each set yields some variation in node ages, but consistent results across all sensitivity analyses (*SI Appendix*, Fig. S9-11, S21-S22). We recommend that researchers use the 'completed' or 'DNA-only' tree sets for addressing questions where diversification rates or trait evolution are paramount, respectively; when that distinction overlaps (e.g., trait-dependent diversification) we recommend comparing analyses run on tree samples from both sets.

Tree-wide and among-clade tempo of lineage diversification. The absolute and relative timings of mammal diversification are debated [23,41], with particular controversies around whether early placentals diverged before, after, or during the Cretaceous-Paleogene (K-Pg) mass extinction event, 66 Ma (short fuse, long fuse, or explosive models, respectively [42]). We estimate the age of crown Placentalia at 92 Ma (95% confidence interval [CI] of 77, 105 using node-dating; tip-dating yielded mostly similar results, *SI Appendix*, Fig. S9). The first four

117 placental divergences unambiguously preceded the K-Pg (Fig. 3a; filled circles), followed by the
118 next 21 divergences with CIs that overlap the K-Pg (Fig. 3a–b). We find a Cretaceous "fuse" of
119 ~25-Ma between the radiation of crown Placentalia and nine of 18 crown orders (*SI Appendix*,
120 Table S6), in line with some estimates [41,43], but longer than others (e.g., [23]). The burst of
121 tree-wide lineage turnover we recover near the K-Pg (visual anomalies in speciation and
122 extinction rates; Fig. 3c) is remarkable for matching concurrent fossil evidence for pulses of
123 origination and extinction [42,44,45] (Fig. 3d). Despite spatiotemporal biases in fossil
124 preservation [46,47] and extant phylogeny reconstruction [48], corroboration between these
125 genetic and fossil data suggests they reflect genuine dynamics in mammalian evolution [49].
126 We recover at least 24 lineage-specific shifts in the net diversification rates of mammals
127 (Fig. 1, 3c, e; shifts present in ≥ 50% of maximum shift credibility trees analyzed in BAMM
128 [50]; see *SI Appendix*, Table S8). The earliest rate shift occurs in either crown Placentalia (1.1x
129 higher than the Mammalia-wide median rate of 0.138 species/lineage/Ma) or Boreoeutheria
130 (1.6x, node C in Fig. 1). These shifts involve 18 different lineages and are all positive, except a
131 rate decrease uncovered for the primate clade of lemurs, lorises, and galagos (Strepsirrhini; node
132 O). The two largest rate increases (4.0x and 3.2x) occurred in the last 10 Ma: the gopher-like
133 tuco-tucos of South America (*Ctenomys*, node Q), and the Indo-Pacific flying foxes (*Pteropus*,
134 node J). Overall, rate increases near the present tend to be particularly high, with a 2.2x mean in
135 the Miocene versus 1.3x in each the Oligocene and Eocene (Fig. 3c; df=2, F=7.772, P=0.003),
136 which corroborates the expectation for extinctions deeper in the tree (e.g., [44]) to have reduced
137 our ability to detect more ancient shifts [48,50]. Different to the explosive model [42], no
138 lineage-specific rate shifts implicate the K-Pg in promoting radiations, either preceding the event
139 (Placentalia) or occurring later (Fig. 3c, e). Notably, we record the highest probability of tree-

wide rate increases ~15 Ma (*SI Appendix*, Fig. S15c and d), in contrast to previous results for rate decreases ~8 and ~3 Ma in mammals [23,26].

Within-clade tempo of lineage diversification. The timings of radiation we recover emphasize that the majority of mammalian diversification in extant lineages occurred during the last ~50 Ma (Fig. 1, 3). Environmental changes during this period are posited to have broadly changed the biosphere [3,51], with potential imprints on phylogenies as temporal variation in diversification rates [4–6,49]. We predicted that species-rich clades would display stronger signatures than depauperate clades of rate-variable (RV) diversification if RV processes were predominant, since the likelihood of rare events (within-clade shifts in speciation or extinction) and our statistical power to detect them should increase with clade size. Rate increases are also expected to yield more extant species. We find that models of RV diversification [49] were favored over rate-constant (RC) models [48] for five out of 12 placental subclades tested (Fig. 3f; *SI Appendix*, Table S9). The strongest RV signal is in the speciose mouse-related clade of rodents, along with shrews, catarrhine primates, and the cow- and whale-related clades of artiodactyls (Fig. 3e), the latter of which was previously suggested [49,50]. However, since we also found lineage-specific rate shifts in those groups (clades 46, 31, 42, 37, and 36; Fig. 1, 3e–f), it was not possible to distinguish between within-lineage scenarios of multiple rate regimes or time-variable rates using these modeling approaches.

As an additional, more sensitive, test of within-clade rate variation, we use clade-wide distributions of tip-level speciation rates as assessed using the tip DR metric [11] (Fig. 3f). We find the overall-highest tip speciation rates in simian primates (clades 42–43), including the human genus *Homo* (80th percentile, median 0.321 species/lineage/Ma; *H. sapiens* and three extinct species) and Indomalayan lutung monkeys (95th percentile, 0.419, *Trachypithecus*), while

163 the distinctive aardvark and platypus have the lowest tip speciation rates (clades 1, 14; Fig. 1).
164 Broadly, we recognize substantial heterogeneity in tip rates across the mammal tree, sometimes
165 with a few high-tip-rate species nested together with low-tip-rate species (Fig. 1), resulting in
166 long right-side tails in the tip rate distributions (positive skew, e.g., clades 38 and 44 in Fig. 1,
167 3f). We find that tip rate skew measures aspects of within-clade speciation rate variation that is
168 otherwise uncaptured by model-fitting approaches (*SI Appendix*, Table S10).

169 **Time and ecology relative to clade species richness.** The relative importance of clade
170 ages (time) versus rates of speciation and extinction (whether stochastic or ecologically driven)
171 as an explanation of extant diversity levels is a matter of intense debate in mammals [5,6,52,8]
172 and other taxa [19,53,27,54]. Past efforts to separate these hypotheses have focused on named
173 clades (e.g., [4]), which are biased by subjective delineation and often vast age differences
174 (mammal families range 3.8–59.0 Ma in mean crown ages; *SI Appendix*, Dataset S7). To avoid
175 this bias, we sliced phylogenies at five-million-year intervals and took the tipward clades as
176 objective units for analysis (Fig. 4a; *SI Appendix*, Fig. S5). Time-sliced clades thus account for
177 the 'pull of the present' in modern trees [55] by analyzing successive levels of rootward
178 covariance among clade crown age, species richness, tip speciation rate mean and skew, and
179 mean ecological traits. If time-constant rates predominate [27,53,56], crown ages will explain
180 most of the among-clade variation in species richness. In contrast, if rate variation is strong, as
181 we already recognized for some nodes and named clades (Fig. 3) and expect from varying
182 ecological regimes [2,5,6,19], diversification rates will have the greater explanatory power.

183 We find that clade age and richness are positively correlated—yet significantly less so
184 than the unique effects of tip speciation rate mean and skew on richness (Fig. 4, multivariate
185 PGLS; *SI Appendix*, Fig. S18 for univariate and taxon-based results). Critically, clade tip rate

mean has stronger effects on richness than expected from simulated RC trees containing only stochastic rate variation (Fig. 4c). Clade tip rate skew is also significant, especially so at deeper time slices (Fig. 4d), confirming that single speed-ups in diversification within a clade (e.g., due to a rate shift in one lineage) can drive much of its overall species richness today. These analyses support arguments that 'ecology' (broadly defined to include anything that alters rate processes) is a greater macroevolutionary force than time [54]; however, both clearly contribute to observed richness (adjusted-R^2: 0.88 full model versus 0.26 with crown age only, means of 100-tree PGLS among 35-Ma clades). Jointly analyzing richness determinants in time-sliced clades offers an objective way to assess age and rate effects that, in turn, enables tests for which ecological factors are driving rate variation.

Linking ecology to uneven diversification and richness. Vagility, latitude, and diurnality are among the key purported causes of variation in mammalian species richness [3,5,6,57]. Species vagility, through its effect on gene-flow patterns [19,58], has been posited as inversely related to the probability and scale of geographic isolation, and hence allopatric speciation [21,59]. However, to our knowledge, vagility has never been assessed for its effects on mammalian speciation rates (see *SI Appendix*, Fig. S7 for an explanation of our allometric index of vagility). We performed phylogenetic path analysis [60] to assess the indirect effects of these ecological factors on mammalian richness via their impact on the joint, yet unequal, contributions of rates and ages to extant species numbers (Fig. 5, *Methods*, *SI Appendix*, Fig. S8). Here, the time-sliced clades allow us to distinguish trait-rate dynamics that are localized near the species level (if traits drive ephemeral speciation [16] or if they evolved very recently) from those that occur deeper in the tree and persist (if traits evolved anciently and did not affect extinction rates). We find that at the species level, and especially in herbivores and carnivores,

209 low-vagility mammals have higher tip speciation rates (Fig. 5a; ecological trait ~ rate PGLS [8]).
210 Effects of vagility on clade tip rate mean are weakened toward deeper time slices, where they are
211 instead recorded on tip rate skew (Fig. 5b). We interpret these short-lived effects of vagility on
212 speciation rates as consistent with expectations that nascent allospecies are produced at a high
213 rate, but are ephemeral, going extinct before their peripheral isolate can expand [16,19,59].
214 While the nearly 20% of mammal species that are endemic to islands complicates our allometric
215 vagility index, we note that the ~10-million-year 'threshold' whereby low-vagility lineages find
216 an adaptive zone, evolve greater vagility, or vanish is robust to multiple sensitivity tests (*SI*
217 *Appendix*, Fig. S21-S22). The influence of vagility on mammal diversification, however, might
218 be non-linear as it is in birds (e.g., humped [19] or sigmoidal [21]).
219 Latitude, through strong covariation with environmental conditions and species richness,
220 is considered to represent key mechanisms behind cross-taxon disparities in richness [3,13]. But
221 recent evidence casts doubt on this presumed negative association between latitude and
222 diversification rates [11,13,14]. Here we find that there is no effect of absolute latitude on tip-
223 level rates of speciation (Fig. 5a). Instead, strong positive associations with latitude arise at
224 deeper time slices, but without corresponding effects on clade tip rate skew (Fig. 5b). Similarly
225 weak latitude-to-rate effects in young clades and species of birds [11,13,14] appear to emphasize
226 the impact on species turnover cycles of temperate climatic instability, seasonality, and
227 expansion of new habitats. We suggest that the traditionally invoked tropical 'cradle' (higher
228 speciation) and 'museum' (lower extinction [3]) should re-focus upon the *combined turnover* of
229 those processes, testing whether extratropical species are 'cycled' faster than tropical species
230 and, if so, relative to which biogeographic processes. Extratropical lineages may not cycle fully,
231 but instead persist through climatic oscillations in glacial refugia [61]. The Eocene-Oligocene

transition (~34 Ma) from tropical to temperate habitats [3] would then have initiated converse latitudinal gradients in species turnover rates and total richness, although North American mammal fossils suggests a steeper richness gradient beginning ~15 Ma [62].

Diurnality is a core behavioral-physiological trait tied to temporal niche innovation [57] and the associated potential for adaptive diversification. We find that repeated origins of daytime activity since the late Eocene (~35 Ma [57,63]) are associated with faster speciation, both at the present (Fig. 5a) and among 10-Ma time-sliced clades (Fig. 4b). Lineage-specific rate regimes also reflect signatures of greater diurnal activity on speciation rates (*SI Appendix*, Fig. S17a). These results affirm the importance of diurnality [63] in the context of other drivers of rate variation (vagility and latitude), placing previous findings of rapid diversification in diurnal lineages of primates [64] in a broader context. Results for 30- and 50-Ma clades appear to be confounded with nocturnal ancestors, including inverse effects on tip rate skew (Fig. 5b), which is consistent with diurnality evolving well after a "nocturnal bottleneck" among K-Pg-surviving mammals [57]. In contrast to vagility and latitude, we posit that greater daytime activity is an example where adaptive divergence in niche traits has decreased extinction rates via competitive release [17], and therefore led to greater persistence and species richness in diurnal lineages.

Conclusions. Our novel, time-calibrated phylogeny addressing all extant and described species of mammals puts a focus on ecological drivers of speciation and diversification. Rate-shifted clades have disparate ecological characteristics (*SI Appendix*, Fig. S17e), suggesting that lineage-specific events have fostered mammalian radiations. Nevertheless, we detect cross-clade signatures of intrinsic (vagility, activity pattern) and extrinsic (latitude) factors driving aspects of diversification at nested phylogenetic levels. We hypothesize that two main processes are at work. First, turnover-mediated diversification is acting on short timescales due to geographic

255 isolation among low-vagility species, and on longer timescales due to the dynamics of
256 extratropical climates. Second, persistence-mediated diversification is demonstrated for diurnal
257 lineages and related more generally to adaptations (or stable habitats) that result in lower
258 extinction rates. Traversing between these modes of diversification may be possible if otherwise
259 ephemeral allospecies can enter novel regions of the phenotype-to-environment landscape, either
260 via niche evolution or extrinsic opportunity [6,16,17,59], to then continue diversifying with
261 lower extinction risk. Overall, we show that ecological factors are influencing speciation rates,
262 but the effects manifest at different hierarchical levels of the tree. Geologically recent processes
263 associated with turnover or adaptation are not yet studied for most of life, but our results in
264 mammals suggest that lineage-level gradients in these novelty-originating processes have causes
265 rooted in the dynamics of population-level gene flow.

Methods

Building new species-level trees for extant Mammalia

Overview. We reconstructed the evolutionary history of extant Mammalia aiming to maximize the accuracy and comparability of temporal information (branch lengths) across lineages in a credible set of time-calibrated phylogenies. Trees were built using a multi-step strategy (Fig. 2) designed to: (i) sample and vet available DNA sequences for extant and recently extinct species into a 31-gene supermatrix; (ii) use an updated taxonomy accounting for 367 new species and 76 genus transfers (5,911 total species; *SI Appendix*, Table S2 and Dataset S2); (iii) estimate a global maximum likelihood (ML) tree for 4,098 species in the DNA supermatrix to inform taxonomic constraints (*SI Appendix*, Dataset S3); (iv) include species unsampled for DNA within the Bayesian phylogenetic analyses (PASTIS completion [65]); and (v) integrate fossil data at nodes and tips to compare methods of calibrating backbone divergence times in mammals. We modified the backbone-and-patch analysis framework [11] to estimate the relative-time phylogenies of 28 non-overlapping subclades of mammals, called "patches" (identified in the global ML tree; Table S5 and Dataset S3). We then re-scaled branches to corresponding divergence times in fossil-calibrated backbones, and grafted the subclade patches to backbones to form Mammalia-wide trees (*SI Appendix*, Fig. S1-S3). We compared trees built using node-dated backbones (17 fossil calibrations [39]) and tip-dated backbones (matrix of modern and Mesozoic mammals [40]), which yielded broadly similar ages (*SI Appendix*, Fig. S9-S11). Strict topology constraints from the global ML tree were used in the 10,000 taxonomically completed trees (5911 species, 'TopoCons') while the DNA-only trees were estimated without topology constraints (4098 species, 'TopoFree').

DNA gathering pipeline. We used the BLAST algorithm (Basic Local Alignment Search Tool [66]) to efficiently query a local copy of NCBI's nucleotide (nt) database, targeting 31 gene fragments (*SI Appendix*, Table S1) commonly sampled among mammals. Meredith et al. [41] was our starting point since their matrix included most extant families for 22 exons and 5 non-coding regions. We further targeted four protein-coding mitochondrial genes to maximize species-level sampling. For each gene, we used a set of pre-vetted sequences or 'baits' as queries for extracting homologous gene fragments from the NCBI database using the "blastn" executable (BLAST+ version 2.2.31) and the XML2 output format to assign taxonomic information for subsequent parsing.

Synonym resolving and master taxonomy for this study. The NCBI taxonomy of our genetic data contained many synonyms that required matching to accepted mammalian species prior to analysis. We based this matchup on a synonym list compiled from Catalogue of Life, MSW3 [67], and IUCN (total of 195,562 unique equivalencies; updated from Meyer et al. [68]). This procedure yielded direct matches for 75% of the NCBI names from our BLAST search. We matched an additional 765 names via manual reference to the literature and identified 1273 species synonyms to yield a list of 4,217 accepted species with ≥1 sampled gene for subsequent error-checking. This taxonomic matchup also produced a master taxonomy of 5911 mammalian species for this study, of which 5,804 species are considered extant (*SI Appendix*, Table S2). The Mammal Diversity Database [69,70] (mammaldiversity.org) was an outgrowth of our project, and continues to update mammalian taxonomy as new literature is published.

DNA sequence error-checking and alignment. We used an iterative per-gene approach to clean annotation errors in NCBI, as follows: (i) sequence alignment, (ii) gene-tree construction

(RAxML v.8.2.3 [71]), and (iii) error-checking for stop codons and insufficient alignment overlap (Fig. 2a). In total, our error-checking steps excluded 1618 sequences across all genes (i.e., 7.2% of the 22,504 individual DNA sequences; *SI Appendix*, Table S1 and S3) corresponding to 119 species, and yielding 4098 species with ≥1 gene fragment validated in the final 31-gene matrix (Dataset S1 lists excluded sequences).

Global DNA-only ML tree. Phylogenetic analysis of the 4098-species DNA matrix was first performed in RAxML with the goal to identify the single best-supported topology for global mammals (*SI Appendix*, Table S4, Dataset S3). The supermatrix of 39,099 base pairs (bp) was 11.9% complete in terms of ungapped sites, which was a level of missing data not expected to confound phylogeny estimation [72,73].

Patch subclades and PASTIS completion of missing species. Examination of well-supported nodes (>75% bootstrap support) in the global ML tree informed our division of the mammalian phylogeny into 28 patch subclades [11]. Delimiting patches was an essential step for conducting Bayesian analyses on manageable tree sizes given that co-estimation upon ~1000 or more species from our DNA supermatrix exceeded reasonable computational limits (*SI Appendix*, Fig. S2, Table S5). Taxonomic constraints for MrBayes v.3.2.6 [74] were formed with the R package PASTIS [65], reducing the potential for human error while identifying non-monophyletic genera in the global ML tree (see Dataset S4). Completed species' branch lengths were drawn from the same birth-death distribution as the rest of the patch clade, tending PASTIS completions conservatively to rate-constant processes while preserving the taxonomically expected tree shape [11,65].

Fossil-dated backbone trees. Two backbones were constructed: (i) node-dating (ND), using 17 fossil calibrations from Benton et al. [39], as augmented by Philips [75]; and (ii) tip-dating (fossilized birth-death, FBD [76]), using the morphological data set of Zhou et al. [40] trimmed to 76 fossil and 22 extant taxa (mostly Mesozoic fossils, 66–252 Ma). In both analyses, we focused on a common set of extant taxa to subset the full supermatrix for molecular characters (59 mammals, representing each of the 28 patch clades plus select family-level taxa with morphological data, and 1 outgroup *Anolis carolinensis*). ND and FBD analyses were conducted in MrBayes analogously to patch clades, and compared to test dating sensitivity (*SI Appendix*, Fig. S9, Table S6, Dataset S5).

Construction of full dated mammalian phylogenies. Tree distributions from the 28 patch subclades (Completed TopoCons and DNA-only TopoFree) and two backbones (ND and FBD) was performed in ape [77], as outlined in the *SI Appendix*. Sets of 10,000 trees will be available in the phylogeny subsetting tool at vertlife.org/phylosubsets and temporarily at XXXX.

Tests for diversification-rate variation or constancy

Tip-level speciation rates. Following ref. [11] we calculated per-species estimates of expected pure-birth diversification rates for the instantaneous present moment (tips of the tree) using the inverse of the equal splits measure [11,12]. This metric has been called 'tip-level diversification rate' (tip DR) because it measures recent diversification processes among extant species [7]. However, to avoid confusion with 'net diversification', for which tip DR is misleading when extinction is very high (relative extinction >0.8 [78]), we here refer to tip DR as a tip-level speciation rate metric. At the tip level, we show that tip DR is tightly associated with model-based estimators of speciation and net diversification rates in our trees (*SI Appendix*, Fig. S4a). At the clade-level, we measure 'clade tip speciation mean' as the harmonic mean of tip DR

among species, which is known to converge to the maximum likelihood estimator of pure-birth diversification rate in clades >10 species [11,12]. We show that clade tip DR mean indeed best approximates pure-birth clade rates for time-sliced clades in our mammal trees (R^2: ~0.7 versus ~0.5 for birth-death speciation and net diversification rates; *SI Appendix*, Fig. S4b).

Lineage-specific rate shifts. We performed searches for macroevolutionary shifts using BAMM v2.5 [50], a reversible-jump algorithm for sampling birth-death scenarios of variable rate regimes without a prior hypothesis. The phylogenetic uncertainty in our trees prompted us to evaluate the number and location of rate shifts on 10 trees from the node-dated sample. We summarized across the most likely shifts per tree—called maximum shift credibility (MSC) sets (*SI Appendix*, Fig. S15a)—using the ratio of the mean net diversification rate of all branches inside the shifted clade (clade rate) and outside that clade (background rate) to calculate the rate shift magnitude and direction for each MSC set (*SI Appendix*, Table S8 and Dataset S7; for tree-wide rate shifts, see *SI Appendix*, Fig. S15-S16).

Fossil diversification. To assess the congruence of our molecular phylogeny-based rate estimates with the fossil record, we analyzed Mammalia fossil occurrence data from the Paleobiology Database [79]. Grouping by genus after excluding ichnotaxa and uncertain genera, we recovered 71,928 occurrences of 5300 genera, which we then binned in 10-Ma intervals and used shareholder quorum subsampling (SQS [80]; quorum size: 0.5) to maximize the uniformity of coverage. Corresponding origination and extinction rates per stage were calculated using the per-capita rate method [81], and the oldest fossil per extant order was compared to stem ages in our node-dated phylogeny (*SI Appendix*, Fig. S13, Table S7).

Likelihood tests of RC and RV models of diversification. We analyzed the branching times of 27 named subclades (11 orders and 16 suborders) that contained ≥25 species. For each subclade, we tested 10 models developed by Morlon et al. [49]: two rate-constant (RC) models, constant PB and BD; and eight rate-variable (RV) models, with exponentially and linearly time-varying rates. We fit models for 100 trees of the empirical subclades and their matching RC-simulated trees (null models, simulated under the empirical extinction fractions of ~ ε=0.65 over 100 trees using the "pbtree" function in phytools [82]). Subtracting AICc scores of the best-fitting RC and RV models provided the $\Delta AIC_{RC\text{-}RV}$ test statistic per tree and subclade for comparison to the simulated null distribution (alpha=0.05; see *SI Appendix*, Table S9).

Time-sliced clades and clade-level PGLS. To objectively define clades, we arbitrarily drew lines (referred to as "time slices") at 5-Ma intervals and took the resulting *tipward* monophyletic clades as non-nested units of analysis. The *rootward* relationships of those clades (the "rootward backbone") was retained for each interval, giving the expected covariance structure among clades when performing phylogenetic generalized least squares (PGLS) analyses (*SI Appendix*, Fig. S5 for illustration). We used the "treeSlice" function in phytools to construct clade sets across Mammalia trees and the three sets of RC simulations, empirical (ε=0.65), low (ε=0.2), and high (ε=0.8), also comparing our results to analyses on traditional taxon-based clades (genera, families, and orders; *SI Appendix*, Fig. S18-S20). All PGLS was performed excluding extinct species, using Pagel's "lambda" transformation in phylolm (optimized for large trees [83]), and repeating the analysis across 100 or 1000 trees.

Tests for causes of diversification-rate variation

Mammalian trait data. Our workflow for gathering trait data involved (i) unifying multiple trait taxonomies (e.g., EltonTraits v1.0 [84]) to our phylogeny's master taxonomy; and

(ii) interpolating home range area and vagility to the species level using known allometric relationships in mammals (*SI Appendix*, Fig. S6, Dataset S7). Vagility was calculated as the maximum natal dispersal distance per individual (km) and interpolated for each species following our updated version of Whitmee and Orme's [85] best-fit equation, testing for collinearity prior to analyses (*SI Appendix*, Fig. S7).

Tip-level correlates of diversification rates. To better understand correlative structures underlying the observed rate variation, we performed tip-level PGLS analyses between species' ecological traits and tip DR values across 1000 trees, focusing on a 5675-species data set that excluded all extinct (n=107) and marine (n=129) species. We followed Freckleton et al. [8] in using trait ~ rate models in our tip-level PGLS analyses to avoid identical residuals in the dependent variable (i.e., sister species have identical tip DR values, violating the assumption of within-variable data independence in bivariate normal distributions). The trait ~ rate approach has been applied using tip DR in univariate contexts [86] (see *SI Appendix*, Fig. S21 for sensitivity tests).

Clade-level correlates of diversification rates. At the clade level, univariate PGLS was performed typically (rate ~ trait models), since clade tip DR mean gave independent values to sister clades. These analyses were conducted on 1000 trees by analogy with those previous, except that per-clade trait summaries were the standardized predictors (geometric means for vagility, otherwise arithmetic means). We also performed tests for trait-dependent diversification using rate-shifted clades identified in BAMM runs on 10 mammal trees (STRAPP [87] method), which corrects for phylogenetic pseudoreplication similar to PGLS except considering only the covariance structure among rate regimes (see *SI Appendix*, Fig. S17).

Phylogenetic path analyses. Path analysis aims to fully resolve correlational structures and thereby translate from the language of statistical probability to causality. In phylogenetic path analyses, we used PGLS to test statements of conditional independence [60] across 27 pre-selected path models (*SI Appendix*, Fig. S8). For each tree and clade set, we used "phylopath" [88] to analyze models and perform conditional model averaging. Time-sliced clades at 10-, 30-, and 50-Ma intervals were analyzed along with taxon-based clades (*SI Appendix*, Fig. S20, S22).

Data availability

All data and code is available in the manuscript, supplementary materials, and after publication on Dryad (all code will be available at github.com/n8upham/).

Acknowledgments

We thank I. Quintero, M. Landis, D. Schluter, A. Mooers, A. Pyron, G. Thomas, D. Greenberg, and E. Florsheim for conceptual discussions that improved this study; B. Patterson, K. Rowe, J. Brown, T. Colston, T. Peterson, D. Field, T. Stewart, J. Davies, and three anonymous reviewers for comments on earlier drafts; S. Upham for improving figure design; C. Meyer for his synonym list; and M. Koo, A. Ranipeta, J. Hart, M. Swanson, C. Burgin, and J. Colella for database help. Artwork from phylopic.org and open source fonts. The NSF VertLife Terrestrial grant to W.J. and J.E. (DEB 1441737 and 1441634) and NSF grant DBI-1262600 to W.J. supported this work.

References

1. Willis JC. Age and Area. Cambridge: Cambridge University Press; 1922.

2. Mooers AO, Heard SB. Inferring Evolutionary Process from Phylogenetic Tree Shape. Q Rev Biol. 1997;72: 31–54.

3. Mittelbach GG, Schemske DW, Cornell HV, Allen AP, Brown JM, Bush MB, et al. Evolution and the latitudinal diversity gradient: speciation, extinction and biogeography. Ecol Lett. 2007;10: 315–331. doi:10.1111/j.1461-0248.2007.01020.x

4. Rabosky DL, Slater GJ, Alfaro ME. Clade age and species richness are decoupled across the eukaryotic tree of life. PLoS Biol. 2012;10: e1001381.

5. Purvis A, Fritz SA, Rodríguez J, Harvey PH, Grenyer R. The shape of mammalian phylogeny: patterns, processes and scales. Philos Trans R Soc Lond B Biol Sci. 2011;366: 2462–2477. doi:10.1098/rstb.2011.0025

6. Simpson GG. The major features of evolution. New York: Columbia Univ Press; 1953.

7. Quintero I, Jetz W. Global elevational diversity and diversification of birds. Nature. 2018;

8. Freckleton RP, Phillimore AB, Pagel M. Relating Traits to Diversification: A Simple Test. Am Nat. 2008;172: 102–115. doi:10.1086/588076

9. Jablonski D. Species Selection: Theory and Data. Annu Rev Ecol Evol Syst. 2008;39: 501–524. doi:10.1146/annurev.ecolsys.39.110707.173510

10. Rabosky DL. Automatic Detection of Key Innovations, Rate Shifts, and Diversity-Dependence on Phylogenetic Trees. PLOS ONE. 2014;9: e89543. doi:10.1371/journal.pone.0089543

11. Jetz W, Thomas GH, Joy JB, Hartmann K, Mooers AO. The global diversity of birds in space and time. Nature. 2012;491: 444–448. doi:10.1038/nature11631

12. Steel M, Mooers A. The expected length of pendant and interior edges of a Yule tree. Appl Math Lett. 2010;23: 1315–1319. doi:10.1016/j.aml.2010.06.021

13. Schluter D, Pennell MW. Speciation gradients and the distribution of biodiversity. Nature. 2017;546: 48–55. doi:10.1038/nature22897

14. Weir JT, Schluter D. The Latitudinal Gradient in Recent Speciation and Extinction Rates of Birds and Mammals. Science. 2007;315: 1574–1576. doi:10.1126/science.1135590

15. Rabosky DL, Chang J, Title PO, Cowman PF, Sallan L, Friedman M, et al. An inverse latitudinal gradient in speciation rate for marine fishes. Nature. 2018; 1. doi:10.1038/s41586-018-0273-1

16. Rosenblum EB, Sarver BAJ, Brown JW, Roches SD, Hardwick KM, Hether TD, et al. Goldilocks Meets Santa Rosalia: An Ephemeral Speciation Model Explains Patterns of Diversification Across Time Scales. Evol Biol. 2012;39: 255–261. doi:10.1007/s11692-012-9171-x

17. Yoder JB, Clancey E, Des Roches S, Eastman JM, Gentry L, Godsoe W, et al. Ecological opportunity and the origin of adaptive radiations. J Evol Biol. 2010;23: 1581–1596.

18. Schluter D. The ecology of adaptive radiation. Oxford, UK: Oxford University Press; 2000.

19. Mayr E. Animal species and evolution. Cambridge, MA: Belknap; 1963.

20. Jablonski D. Larval ecology and macroevolution in marine invertebrates. Bull Mar Sci. 1986;39: 565–587.

21. Claramunt S, Derryberry EP, Remsen JV, Brumfield RT. High dispersal ability inhibits speciation in a continental radiation of passerine birds. Proc R Soc Lond B Biol Sci. 2012;279: 1567–1574. doi:10.1098/rspb.2011.1922

22. Bininda-Emonds ORP. The evolution of supertrees. Trends Ecol Evol. 2004;19: 315–322. doi:10.1016/j.tree.2004.03.015

23. Bininda-Emonds ORP, Cardillo M, Jones KE, MacPhee RDE, Beck RMD, Grenyer R, et al. The delayed rise of present-day mammals. Nature. 2007;446: 507–512. doi:10.1038/nature05634

24. Fritz SA, Bininda-Emonds ORP, Purvis A. Geographical variation in predictors of mammalian extinction risk: big is bad, but only in the tropics. Ecol Lett. 2009;12: 538–549. doi:10.1111/j.1461-0248.2009.01307.x

25. Kuhn TS, Mooers AØ, Thomas GH. A simple polytomy resolver for dated phylogenies. Methods Ecol Evol. 2011;2: 427–436. doi:10.1111/j.2041-210X.2011.00103.x

26. Stadler T. Mammalian phylogeny reveals recent diversification rate shifts. Proc Natl Acad Sci. 2011;108: 6187–6192. doi:10.1073/pnas.1016876108

27. Hedges SB, Marin J, Suleski M, Paymer M, Kumar S. Tree of life reveals clock-like speciation and diversification. Mol Biol Evol. 2015; msv037. doi:10.1093/molbev/msv037

28. Faurby S, Svenning J-C. A species-level phylogeny of all extant and late Quaternary extinct mammals using a novel heuristic-hierarchical Bayesian approach. Mol Phylogenet Evol. 2015;84: 14–26. doi:10.1016/j.ympev.2014.11.001

29. Marin J, Rapacciuolo G, Costa GC, Graham CH, Brooks TM, Young BE, et al. Evolutionary time drives global tetrapod diversity. Proc R Soc B. 2018;285: 20172378. doi:10.1098/rspb.2017.2378

504 30. Tonini JFR, Beard KH, Ferreira RB, Jetz W, Pyron RA. Fully-sampled phylogenies of
505 squamates reveal evolutionary patterns in threat status. Biol Conserv. 2016;204: 23–31.
506 doi:10.1016/j.biocon.2016.03.039

507 31. Jetz W, Pyron RA. The interplay of past diversification and evolutionary isolation with
508 present imperilment across the amphibian tree of life. Nat Ecol Evol. 2018;

509 32. Rabosky DL, Mitchell JS, Chang J. Is BAMM Flawed? Theoretical and Practical Concerns
510 in the Analysis of Multi-Rate Diversification Models. Syst Biol. 2017;66: 477–498.
511 doi:10.1093/sysbio/syx037

512 33. Moore BR, Höhna S, May MR, Rannala B, Huelsenbeck JP. Critically evaluating the theory
513 and performance of Bayesian analysis of macroevolutionary mixtures. Proc Natl Acad Sci.
514 2016;113: 9569–9574. doi:10.1073/pnas.1518659113

515 34. Beaulieu JM, O'Meara BC. Extinction can be estimated from moderately sized molecular
516 phylogenies. Evolution. 2015;69: 1036–1043. doi:10.1111/evo.12614

517 35. Rabosky DL. Extinction rate should not be estimated from molecular phylogenies.
518 Evolution. 2010;64: 1816–1824.

519 36. Rabosky DL, Goldberg EE. Model Inadequacy and Mistaken Inferences of Trait-Dependent
520 Speciation. Syst Biol. 2015;64: 340–355. doi:10.1093/sysbio/syu131

521 37. Beaulieu JM, O'Meara BC. Detecting Hidden Diversification Shifts in Models of Trait-
522 Dependent Speciation and Extinction. Syst Biol. 2016;65: 583–601.
523 doi:10.1093/sysbio/syw022

524 38. Hodges SA, Arnold ML. Spurring plant diversification: are floral nectar spurs a key
525 innovation? Proc R Soc Lond B Biol Sci. 1995;262: 343–348.

526 39. Benton MJ, Donoghue PCJ, Asher RJ, Friedman M, Near TJ, Vinther J. Constraints on the
527 timescale of animal evolutionary history. Palaeontol Electron. 2015;18.

528 40. Zhou C-F, Wu S, Martin T, Luo Z-X. A Jurassic mammaliaform and the earliest mammalian
529 evolutionary adaptations. Nature. 2013;500: 163–167. doi:10.1038/nature12429

530 41. Meredith RW, Janečka JE, Gatesy J, Ryder OA, Fisher CA, Teeling EC, et al. Impacts of the
531 Cretaceous Terrestrial Revolution and KPg Extinction on Mammal Diversification.
532 Science. 2011;334: 521–524. doi:10.1126/science.1211028

533 42. Archibald JD, Deutschman DH. Quantitative Analysis of the Timing of the Origin and
534 Diversification of Extant Placental Orders. J Mamm Evol. 2001;8: 107–124.
535 doi:10.1023/A:1011317930838

536 43. dos Reis M, Inoue J, Hasegawa M, Asher RJ, Donoghue PCJ, Yang Z. Phylogenomic
537 datasets provide both precision and accuracy in estimating the timescale of placental

538 mammal phylogeny. Proc R Soc Lond B Biol Sci. 2012;279: 3491–3500.
539 doi:10.1098/rspb.2012.0683

540 44. Grossnickle DM, Newham E. Therian mammals experience an ecomorphological radiation
541 during the Late Cretaceous and selective extinction at the K–Pg boundary. Proc R Soc B.
542 2016;283: 20160256. doi:10.1098/rspb.2016.0256

543 45. Pires MM, Rankin BD, Silvestro D, Quental TB. Diversification dynamics of mammalian
544 clades during the K–Pg mass extinction. Biol Lett. 2018;14: 20180458.
545 doi:10.1098/rsbl.2018.0458

546 46. Kalmar A, Currie DJ. The Completeness of the Continental Fossil Record and Its Impact on
547 Patterns of Diversification. Paleobiology. 2010;36: 51–60.

548 47. Alroy J. The Fossil Record of North American Mammals: Evidence for a Paleocene
549 Evolutionary Radiation. Syst Biol. 1999;48: 107–118. doi:10.1080/106351599260472

550 48. Nee S, May RH, Harvey PH. The reconstructed evolutionary process. Philos Trans R Soc
551 Lond B-Biol Sci. 1994;344: 305–311.

552 49. Morlon H, Parsons TL, Plotkin JB. Reconciling molecular phylogenies with the fossil record.
553 Proc Natl Acad Sci. 2011;108: 16327–16332. doi:10.1073/pnas.1102543108

554 50. Rabosky DL. Automatic detection of key innovations, rate shifts, and diversity-dependence
555 on phylogenetic trees. PLoS ONE. 2014;9: e89543.

556 51. Katz ME, Miller KG, Wright JD, Wade BS, Browning JV, Cramer BS, et al. Stepwise
557 transition from the Eocene greenhouse to the Oligocene icehouse. Nat Geosci. 2008;1: 329–
558 334. doi:10.1038/ngeo179

559 52. Venditti C, Meade A, Pagel M. Multiple routes to mammalian diversity. Nature. 2011;479:
560 393–396. doi:10.1038/nature10516

561 53. Ricklefs RE. Global diversification rates of passerine birds. Proc R Soc Lond B-Biol Sci.
562 2003;270: 2285–2291.

563 54. Price TD. The roles of time and ecology in the continental radiation of the Old World leaf
564 warblers (*Phylloscopus* and *Seicercus*). Philos Trans R Soc Lond B Biol Sci. 2010;365:
565 1749–1762. doi:10.1098/rstb.2009.0269

566 55. Nee S, Holmes EC, May RM, Harvey PH. Extinction rates can be estimated from molecular
567 phylogenies. Philos Trans R Soc Lond B-Biol Sci. 1994;344: 77–82.

568 56. Venditti C, Meade A, Pagel M. Phylogenies reveal new interpretation of speciation and the
569 Red Queen. Nature. 2010;463: 349–352. doi:10.1038/nature08630

570 57. Gerkema MP, Davies WIL, Foster RG, Menaker M, Hut RA. The nocturnal bottleneck and
571 the evolution of activity patterns in mammals. Proc R Soc B. 2013;280: 20130508.
572 doi:10.1098/rspb.2013.0508

573 58. Kisel Y, Barraclough TG. Speciation Has a Spatial Scale That Depends on Levels of Gene
574 Flow. Am Nat. 2010;175: 316–334. doi:10.1086/650369

575 59. Jablonski D. Heritability at the Species Level: Analysis of Geographic Ranges of Cretaceous
576 Mollusks. Science. 1987;238: 360–363. doi:10.1126/science.238.4825.360

577 60. von Hardenberg A, Gonzalez-Voyer A. Disentangling Evolutionary Cause-Effect
578 Relationships with Phylogenetic Confirmatory Path Analysis. Evolution. 2013;67: 378–
579 387. doi:10.1111/j.1558-5646.2012.01790.x

580 61. Hewitt G. The genetic legacy of the Quaternary ice ages. Nature. 2000;405: 907–913.
581 doi:10.1038/35016000

582 62. Marcot JD, Fox DL, Niebuhr SR. Late Cenozoic onset of the latitudinal diversity gradient of
583 North American mammals. Proc Natl Acad Sci. 2016;113: 7189–7194.
584 doi:10.1073/pnas.1524750113

585 63. Maor R, Dayan T, Ferguson-Gow H, Jones KE. Temporal niche expansion in mammals from
586 a nocturnal ancestor after dinosaur extinction. Nat Ecol Evol. 2017;1: 1889.
587 doi:10.1038/s41559-017-0366-5

588 64. Arbour JH, Santana SE. A major shift in diversification rate helps explain macroevolutionary
589 patterns in primate species diversity. Evolution. 2017;71: 1600–1613.
590 doi:10.1111/evo.13237

591 65. Thomas GH, Hartmann K, Jetz W, Joy JB, Mimoto A, Mooers AO. PASTIS: an R package
592 to facilitate phylogenetic assembly with soft taxonomic inferences. Methods Ecol Evol.
593 2013;4: 1011–1017. doi:10.1111/2041-210X.12117

594 66. Altschul SF, Madden TL, Schaffer AA, Zhang J, Zhang Z, Miller W, et al. Gapped BLAST
595 and PSI-BLAST: a new generation of protein database search programs. Nucleic Acids Res.
596 1997;25: 3389–3402.

597 67. Wilson DE, Reeder DM. Mammal species of the world: a taxonomic and geographic
598 reference, 3rd ed. 3rd ed. Baltimore, MD: Johns Hopkins University Press; 2005.

599 68. Meyer C, Kreft H, Guralnick R, Jetz W. Global priorities for an effective information basis
600 of biodiversity distributions. Nat Commun. 2015;6: 8221. doi:10.1038/ncomms9221

601 69. Burgin CJ, Colella JP, Kahn PL, Upham NS. How many species of mammals are there? J
602 Mammal. 2018;99: 1–14. doi:10.1093/jmammal/gyx147

603 70. Mammal Diversity Database. American Society of Mammalogists, Mammal Diversity
604 Database [Internet]. 2018 [cited 2 Jun 2018]. Available: https://mammaldiversity.org/

605 71. Stamatakis A. RAxML version 8: a tool for phylogenetic analysis and post-analysis of large
606 phylogenies. Bioinformatics. 2014;30: 1312–1313. doi:10.1093/bioinformatics/btu033

607 72. Wiens JJ, Morrill MC. Missing Data in Phylogenetic Analysis: Reconciling Results from
608 Simulations and Empirical Data. Syst Biol. 2011; syr025. doi:10.1093/sysbio/syr025

609 73. Roure B, Baurain D, Philippe H. Impact of Missing Data on Phylogenies Inferred from
610 Empirical Phylogenomic Data Sets. Mol Biol Evol. 2013;30: 197–214.
611 doi:10.1093/molbev/mss208

612 74. Ronquist F, Teslenko M, Mark P van der, Ayres DL, Darling A, Höhna S, et al. MrBayes
613 3.2: Efficient Bayesian Phylogenetic Inference and Model Choice across a Large Model
614 Space. Syst Biol. 2012; sys029. doi:10.1093/sysbio/sys029

615 75. Phillips MJ. Four mammal fossil calibrations: balancing competing palaeontological and
616 molecular considerations. Palaeontol Electron. 2015;18: 1–16.
617 doi:https://doi.org/10.26879/490

618 76. Heath TA, Huelsenbeck JP, Stadler T. The fossilized birth–death process for coherent
619 calibration of divergence-time estimates. Proc Natl Acad Sci. 2014;111: E2957–E2966.
620 doi:10.1073/pnas.1319091111

621 77. Paradis E, Claude J, Strimmer K. APE: Analyses of Phylogenetics and Evolution in R
622 language. Bioinformatics. 2004;20: 289–290.

623 78. Title PO, Rabosky D. Tip rates, phylogenies and diversification: what are we estimating, and
624 how good are the estimates? bioRxiv. 2018; 369124. doi:10.1101/369124

625 79. Alroy J, Uhen MD, Mannion PD, Jaramillo C, Carrano MT, van den Hoek Ostende LW.
626 Taxonomic occurrences of Mammalia recorded in Fossilworks, the Evolution of Terrestrial
627 Ecosystems database, and the Paleobiology Database. Fossilworks. http://fossilworks.org.
628 2018;

629 80. Alroy J. Accurate and precise estimates of origination and extinction rates. Paleobiology.
630 2014;40: 374–397. doi:10.1666/13036

631 81. Foote M. Origination and extinction components of taxonomic diversity: general problems.
632 Paleobiology. 2000;26: 74–102. doi:10.1666/0094-8373(2000)26[74:OAECOT]2.0.CO;2

633 82. Revell LJ. phytools: an R package for phylogenetic comparative biology (and other things).
634 Methods Ecol Evol. 2012;3: 217–223.

635 83. Ho LST, Ané C. A Linear-Time Algorithm for Gaussian and Non-Gaussian Trait Evolution
636 Models. Syst Biol. 2014;63: 397–408. doi:10.1093/sysbio/syu005

637 84. Wilman H, Belmaker J, Simpson J, de la Rosa C, Rivadeneira MM, Jetz W. EltonTraits 1.0:
638 Species-level foraging attributes of the world's birds and mammals. Ecology. 2014;95:
639 2027–2027. doi:10.1890/13-1917.1

640 85. Whitmee S, Orme CDL. Predicting dispersal distance in mammals: a trait-based approach. J
641 Anim Ecol. 2013;82: 211–221. doi:10.1111/j.1365-2656.2012.02030.x

642 86. Harvey MG, Seeholzer GF, Smith BT, Rabosky DL, Cuervo AM, Brumfield RT. Positive
643 association between population genetic differentiation and speciation rates in New World
644 birds. Proc Natl Acad Sci. 2017;114: 6328–6333. doi:10.1073/pnas.1617397114

645 87. Rabosky DL, Huang H. A Robust Semi-Parametric Test for Detecting Trait-Dependent
646 Diversification. Syst Biol. 2016;65: 181–193. doi:10.1093/sysbio/syv066

647 88. van der Bijl W. phylopath: Easy phylogenetic path analysis in R. PeerJ. 2018;6: e4718.
648 doi:10.7717/peerj.4718

649

Figure legends

Fig. 1. Species-level relationships and tempo of diversification across mammals. The node-dated analysis of 5911 species shows branches colored with tip-level speciation rates (tip DR metric) and marked with 24 shifts in lineage-specific diversification rates (labels A-X; shifts with multiple circles occurred on either branch, not both). Tip-level rates are reconstructed to interior branches using Brownian motion for visual purposes only. The maximum clade credibility topology of 10,000 trees is shown, and numbered clade labels correspond to orders and subclades listed in the plot periphery: Mars, Marsupialia; X, Xenarthra; Afro, Afrotheria; Laur, Laurasiatheria; Euar, Euarchontoglires. Scale in millions of years, Ma.

Fig. 2. Building the backbone-and-patch Mammalia phylogenies. (a) Schematic overview of DNA sequence gathering from NCBI, taxonomic matchup, iterative error checking, and estimating a global maximum-likelihood (ML) tree from the resulting supermatrix (31 genes by 4098 species [71]). Subclade (patch) phylogenies were then delimited, estimated using Bayesian inference [74], and joined to fossil-calibrated backbone trees (node- or tip-dated). The resulting posterior samples of 10,000 fully dated phylogenies either had the global ML tree topology constrained (completed trees of 5911 species, 'TopoCons') or no topology constraints (DNA-only trees, 'TopoFree'). (b) Backbone trees contained topological and age uncertainty, including the unresolved base of Placentalia (e.g., [41]), slightly favoring the Atlantogenata hypothesis (blue) versus Exafroplacentalia (red). (c) Bayesian phylogenies of 28 patch clades were separately estimated in relative-time units for re-scaling to representative divergence times on the backbone. Combining sets of backbones and patch clades yielded four posterior distributions for analysis (see *SI Appendix*, Fig. S9-12).

Fig. 3. Diversification rate variation among mammal clades. Lineage-through-time plots and estimated crown ages for (**a**) all superordinal divergences, and (**b**) placental orders with crown age estimates overlapping the Cretaceous-Paleogene extinction event (K-Pg, dashed gray line; means and 95% CIs; filled circle if statistically different). (**c**) Rate-through-time plots for speciation, extinction, and net diversification (summarized from Fig. 1 rate shifts; medians from 10 trees, 95% CIs in light gray). (**d**) Fossil genus diversity through time for all Mammalia, including subsampled genus richness (quorum 0.5) and per-capita rates of genus origination and extinction. (**e**) Extant rates and lineage-specific rate shifts for the five most speciose mammal orders (same symbols as in **c**). (**f**) Rate variation within subclades of these five orders as numbered from Fig. 1; left: difference in AIC between best-fit models of diversification for trees simulated under rate-constant birth-death (gray) versus observed mammal trees (color; filled circle and * if ΔAIC on 100 trees is statistically different); and, right: tip-level speciation rate (tip DR metric) distributions of the same simulated and observed subclades (gray versus color, one tree), comparing variation in clade tip rate mean and skew across 100 trees. The last 2 Ma are removed from parts **c-e** for clarity.

Fig. 4. Age and rate components of species richness variation across time-slice defined clades. (a) The log species richness of clades tipward of each 5-Ma time slice (dotted lines from 5-70 Ma) across a sample of 100 phylogenies (maximum clade credibility tree shown) is best predicted jointly by (**b**) clade crown age, (**c**) the clade harmonic mean of tip speciation rates (tip DR mean), and (**d**) the clade skew of tip speciation rates (tip DR skew). Multivariate phylogenetic analyses of clade richness in observed trees (gray) is compared to trees simulated under rate-constant birth and death with different extinction fractions, ε (colors in legend; PGLS on standardized data with 95% confidence intervals [CIs] on parameter estimates). Solid black

lines are the observed best-fitting models given random effects of time slice and tree. Insets (**b** to **d**) are examples from 35-Ma clades (red line) showing the bivariate plots underlying each multivariate PGLS slope per tree and time slice.

Fig. 5. Ecological drivers of (a) tip speciation rates and (b) clade speciation rates and species richness. (**a**, top panel) Distribution of tip-level speciation rates (tip DR metric, harmonic mean of 10,000 trees) relative to per-species estimates of vagility (maximum natal dispersal distance), diurnality (0=nocturnal or cathemeral, 1=diurnal), and absolute value of latitude (centroid of expert maps) across 5,675 species (excluding extinct and marine species). Loess smoothing lines visualize general trends (blue, span=0.33). Tip-level effects (bottom panel) from univariate PGLS between tip speciation rates and ecological traits subset across trophic levels (1000 trees, 95% CI, colored if significant). (**b**) Phylogenetic path analysis [60] of putative causal relationships between traits and rates leading to clade species richness for time-sliced clades. Path thickness, color, and directionality denote median coefficients of model-averaged analyses. The bottom panels provide per-estimate uncertainty across time slices (slope ± SE, 1000 trees). Non-zero estimates, either positive (blue shades) or negative (red shades), are totaled in the right margin; paths present in >500 trees are bolded and displayed in path model whereas others are dashed.

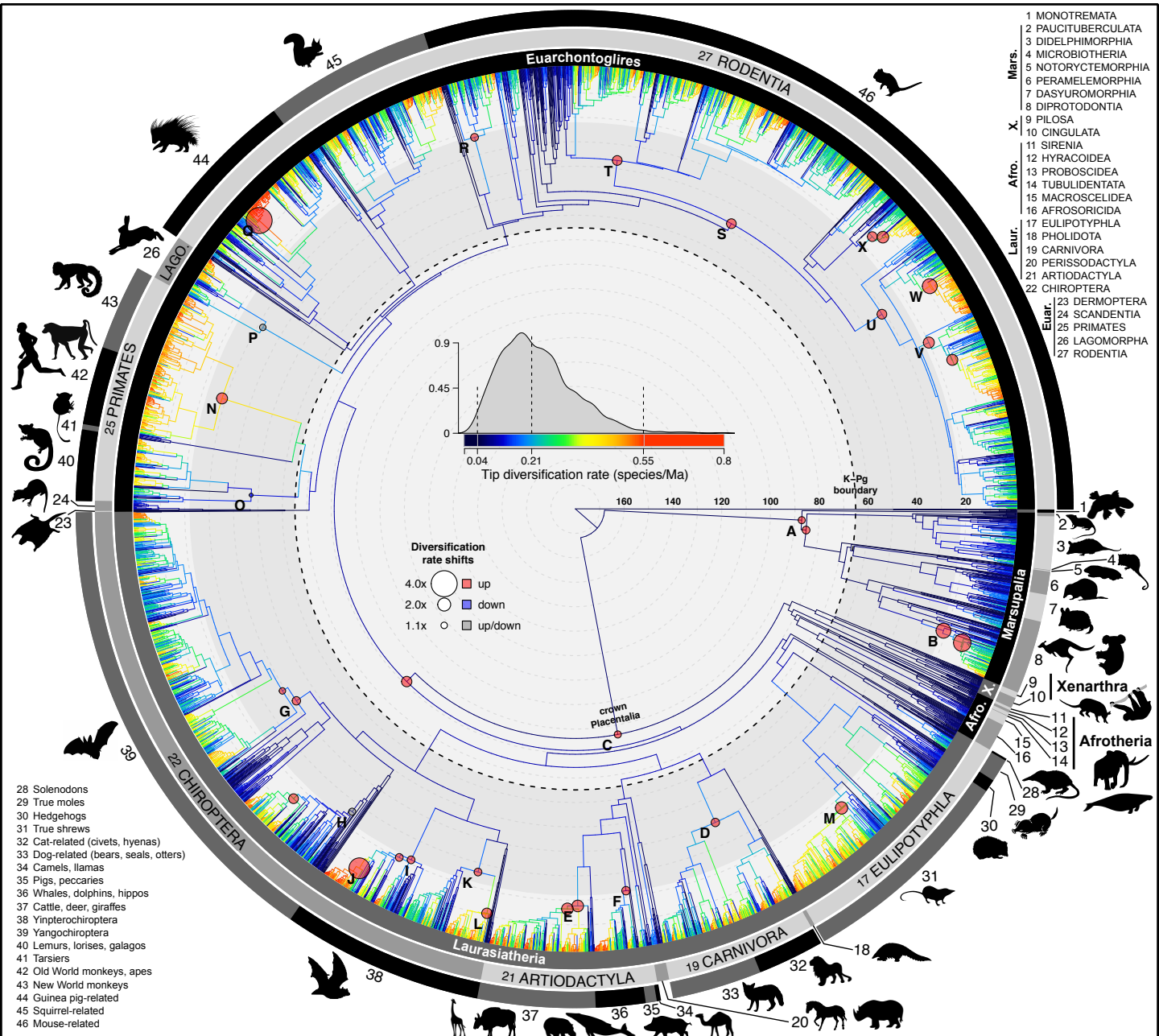

Mars.
1 MONOTREMATA
2 PAUCITUBERCULATA
3 DIDELPHIMORPHIA
4 MICROBIOTHERIA
5 NOTORYCTEMORPHIA
6 PERAMELEMORPHIA
7 DASYUROMORPHIA
8 DIPROTODONTIA

X.
9 PILOSA
10 CINGULATA

Afro.
11 SIRENIA
12 HYRACOIDEA
13 PROBOSCIDEA
14 TUBULIDENTATA
15 MACROSCELIDEA
16 AFROSORICIDA

Laur.
17 EULIPOTYPHLA
18 PHOLIDOTA
19 CARNIVORA
20 PERISSODACTYLA
21 ARTIODACTYLA
22 CHIROPTERA

Euar.
23 DERMOPTERA
24 SCANDENTIA
25 PRIMATES
26 LAGOMORPHA
27 RODENTIA

28 Solenodons
29 True moles
30 Hedgehogs
31 True shrews
32 Cat-related (civets, hyenas)
33 Dog-related (bears, seals, otters)
34 Camels, llamas
35 Pigs, peccaries
36 Whales, dolphins, hippos
37 Cattle, deer, giraffes
38 Yinpterochiroptera
39 Yangochiroptera
40 Lemurs, lorises, galagos
41 Tarsiers
42 Old World monkeys, apes
43 New World monkeys
44 Guinea pig-related
45 Squirrel-related
46 Mouse-related

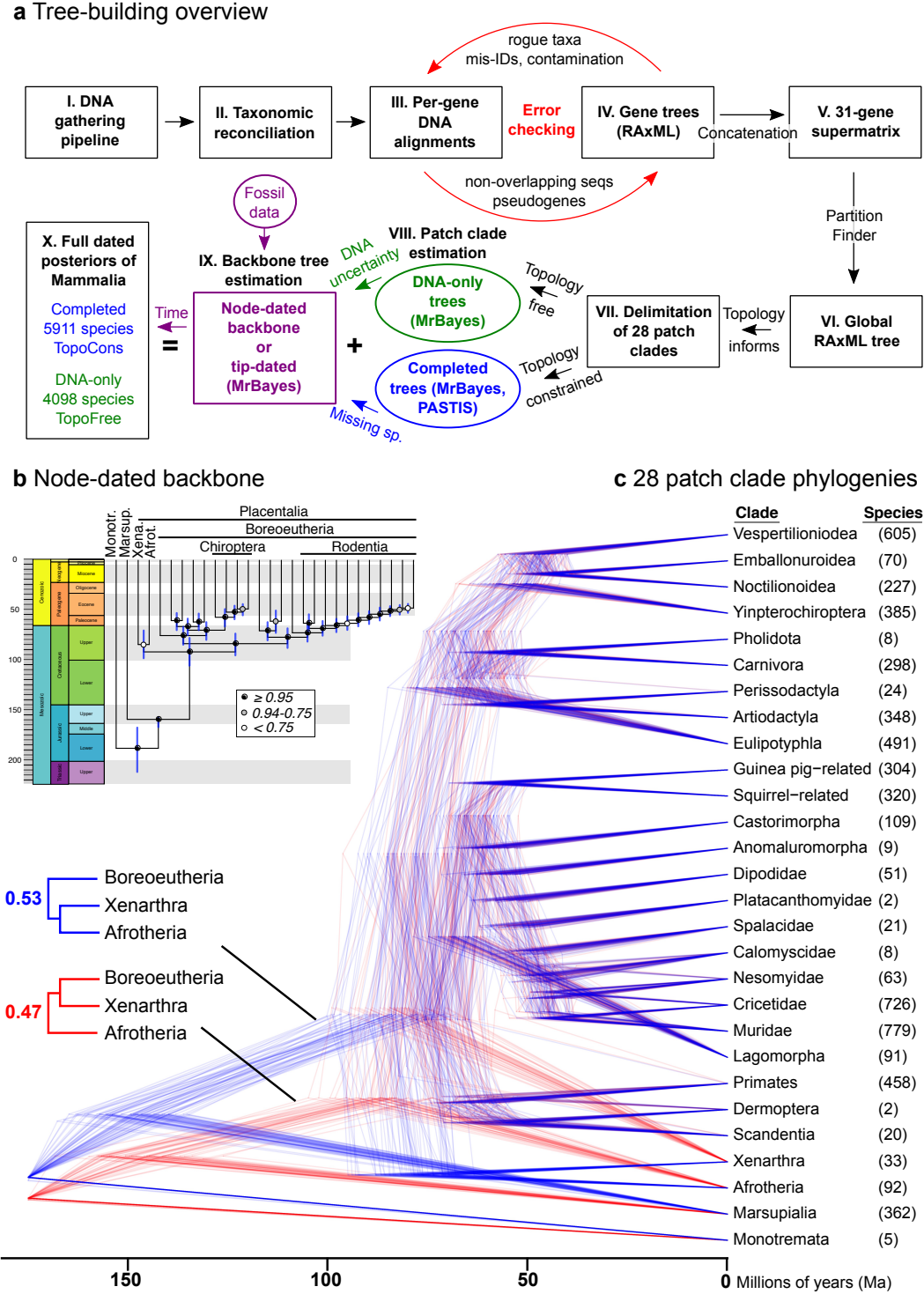
a Tree-building overview
rogue taxa
mis-IDs, contamination
I. DNA gathering pipeline
II. Taxonomic reconciliation
III. Per-gene DNA alignments
Error checking
IV. Gene trees (RAxML)
Concatenation
V. 31-gene supermatrix
non-overlapping seqs
pseudogenes
Partition Finder
Fossil data
X. Full dated posteriors of Mammalia
Completed 5911 species TopoCons
DNA-only 4098 species TopoFree
IX. Backbone tree estimation
Time
=
Node-dated backbone or tip-dated (MrBayes)
+
DNA uncertainty
VIII. Patch clade estimation
DNA-only trees (MrBayes)
Topology free
Completed trees (MrBayes, PASTIS)
Topology constrained
Missing sp.
VII. Delimitation of 28 patch clades
Topology informs
VI. Global RAxML tree
b Node-dated backbone
Monotr.
Marsup.
Xena.
Afrot.
Placentalia
Boreoeutheria
Chiroptera
Rodentia
≥ 0.95
0.94-0.75
< 0.75
c 28 patch clade phylogenies
Clade
Species
Vespertilionioidea (605)
Emballonuroidea (70)
Noctilionoidea (227)
Yinpterochiroptera (385)
Pholidota (8)
Carnivora (298)
Perissodactyla (24)
Artiodactyla (348)
Eulipotyphla (491)
Guinea pig−related (304)
Squirrel−related (320)
Castorimorpha (109)
Anomaluromorpha (9)
Dipodidae (51)
Platacanthomyidae (2)
Spalacidae (21)
Calomyscidae (8)
Nesomyidae (63)
Cricetidae (726)
Muridae (779)
Lagomorpha (91)
Primates (458)
Dermoptera (2)
Scandentia (20)
Xenarthra (33)
Afrotheria (92)
Marsupialia (362)
Monotremata (5)
0.53
Boreoeutheria
Xenarthra
Afrotheria
0.47
Boreoeutheria
Xenarthra
Afrotheria
150
100
50
0
Millions of years (Ma)

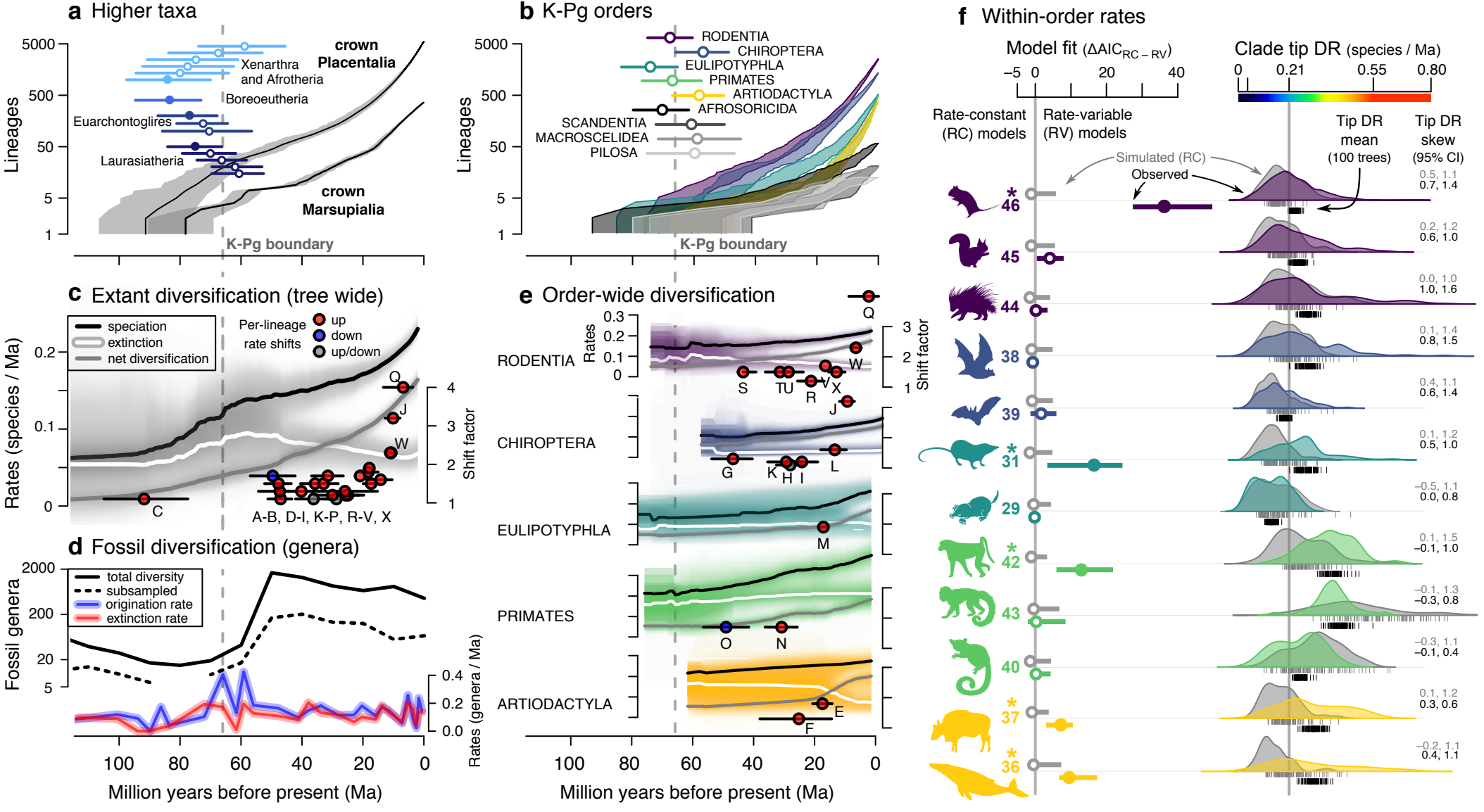
a Higher taxa
Lineages
5000
500
50
5
1
crown Placentalia
Xenarthra and Afrotheria
Boreoeutheria
Euarchontoglires
Laurasiatheria
crown Marsupialia
K-Pg boundary
b K-Pg orders
RODENTIA
CHIROPTERA
EULIPOTYPHLA
PRIMATES
ARTIODACTYLA
AFROSORICIDA
SCANDENTIA
MACROSCELIDEA
PILOSA
c Extant diversification (tree wide)
speciation
extinction
net diversification
Per-lineage rate shifts
up
down
up/down
Rates (species / Ma)
Shift factor
A-B, D-I, K-P, R-V, X
d Fossil diversification (genera)
total diversity
subsampled
origination rate
extinction rate
Fossil genera
Rates (genera / Ma)
Million years before present (Ma)
e Order-wide diversification
Rates
Shift factor
RODENTIA
CHIROPTERA
EULIPOTYPHLA
PRIMATES
ARTIODACTYLA
Million years before present (Ma)
f Within-order rates
Model fit (ΔAIC RC – RV)
Clade tip DR (species / Ma)
Rate-constant (RC) models
Rate-variable (RV) models
Tip DR mean (100 trees)
Tip DR skew (95% CI)
Simulated (RC)
Observed
46
45
44
38
39
31
29
42
43
40
37
36

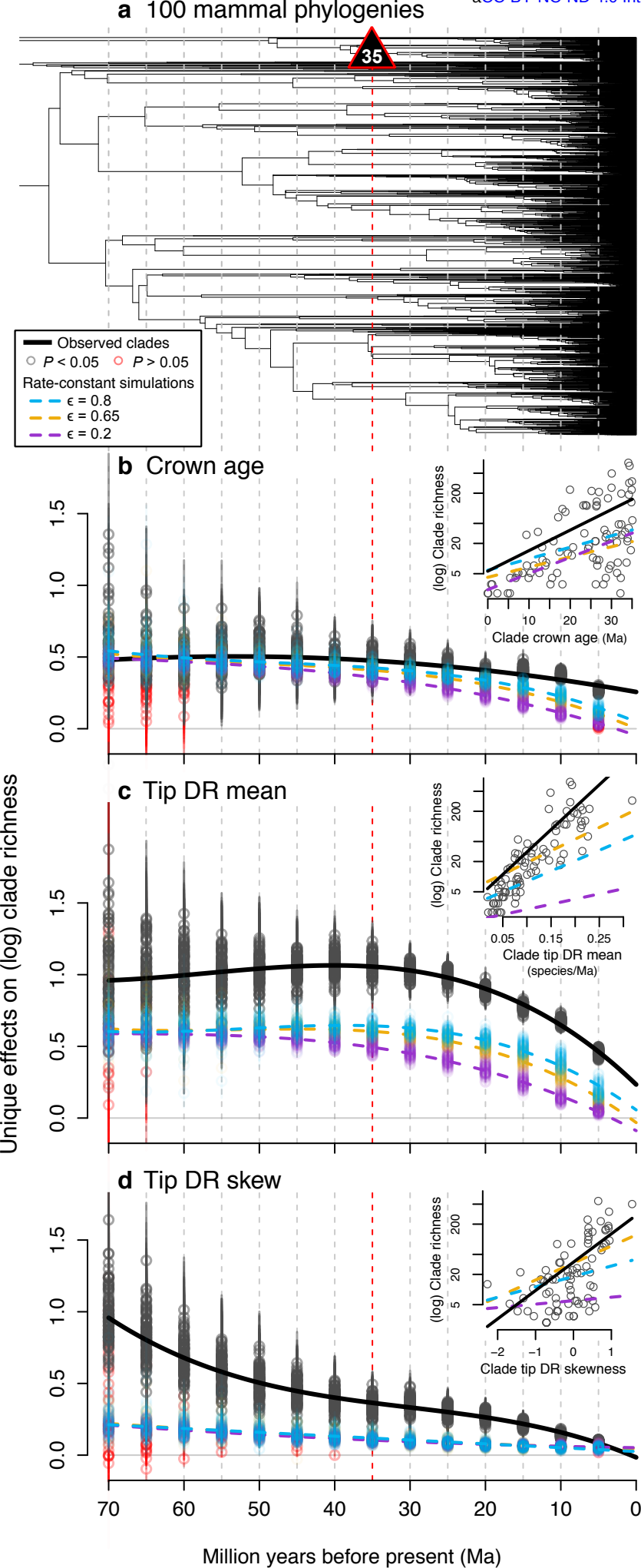

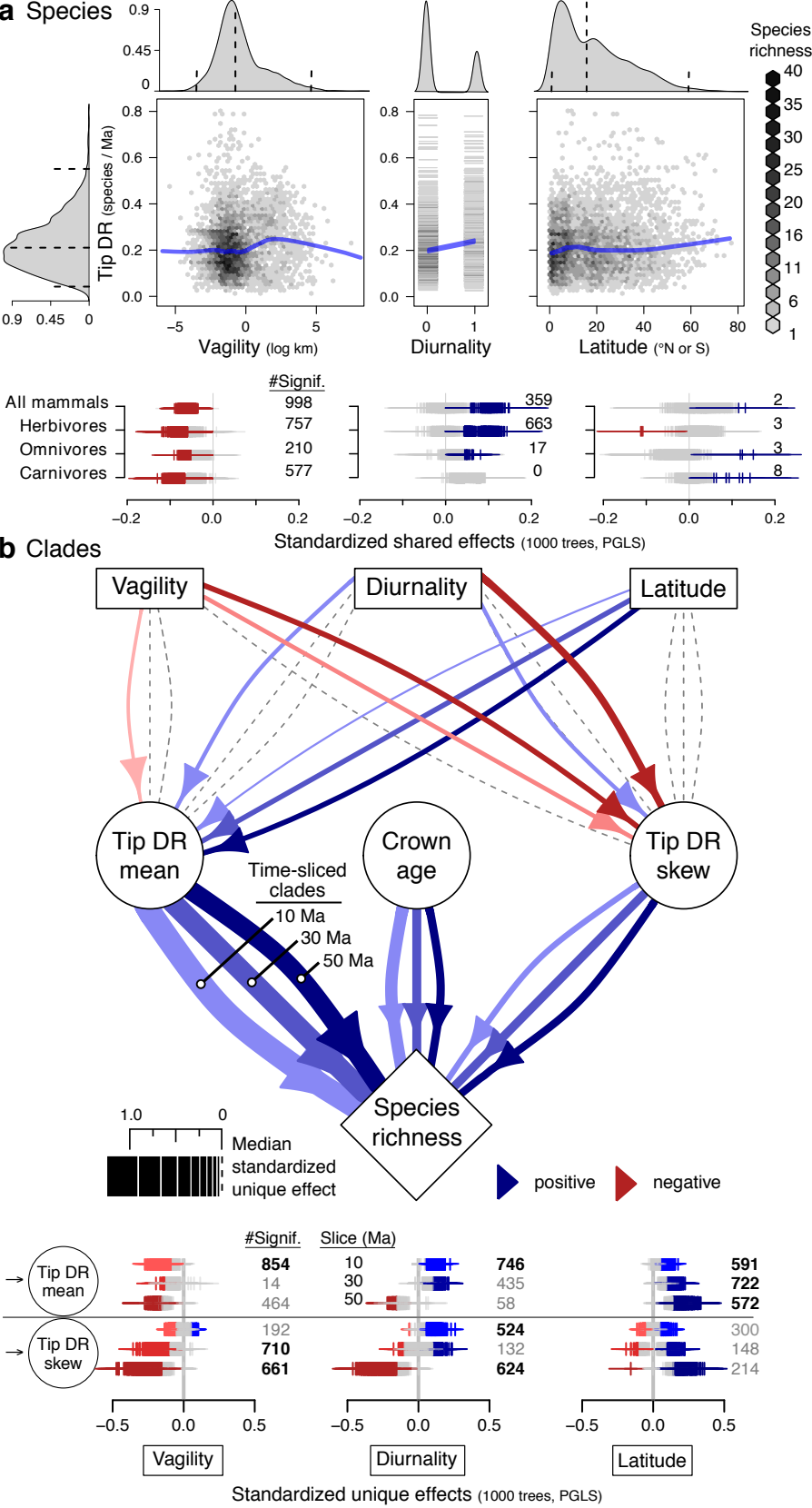
a Species
Tip DR (species / Ma)
Vagility (log km)
Diurnality
Latitude (°N or S)
Species richness
#Signif.
All mammals
Herbivores
Omnivores
Carnivores
998
757
210
577
359
663
17
0
2
3
3
8
Standardized shared effects (1000 trees, PGLS)
b Clades
Vagility
Diurnality
Latitude
Tip DR mean
Crown age
Tip DR skew
Time-sliced clades
10 Ma
30 Ma
50 Ma
Species richness
Median standardized unique effect
positive
negative
#Signif.
Slice (Ma)
Tip DR mean
Tip DR skew
854
14
464
192
710
661
10
30
50
746
435
58
524
132
624
591
722
572
300
148
214
Vagility
Diurnality
Latitude
Standardized unique effects (1000 trees, PGLS)